The magnetism in tectonically controlled travertine as a palaeoseismological tool: examples from the Sıcak Çermik geothermal field, central Turkey

H. GÜRSOY[1], B. L. MESCI[1], J. D. A. PIPER[2], O. TATAR[1] & C. J. DAVIES[2]

[1]*Department of Geology, Cumhuriyet University, 58140 Sivas, Turkey (e-mail: gursoy@cumhuriyet.edu.tr)*

[2]*Geomagnetism Laboratory, Department of Earth and Ocean Sciences, University of Liverpool, Liverpool L69 7ZE, UK*

Abstract: In regions of neotectonic activity geothermal waters flow into extensional fissures and deposit successive layers of carbonate as fissure travertine incorporating small amounts of ferromagnetic grains. The same waters spill out onto the surface to deposit bedded travertine, which may also incorporate wind-blown dust with a ferromagnetic component. Travertine deposits are linked to earthquake activity because geothermal reservoirs are reset and activated by earthquake fracturing but tend to become sealed by deposition of carbonate between events. A weak ferromagnetism records the ambient field at the time of deposition and sequential deposition can identify cycles of secular variation of the geomagnetic field to provide a means of estimating the rate of travertine growth. The palaeomagnetic record in three travertine fissures from the Sıcak Çermik geothermal field in central Anatolia dated to between 100 and 360 ka by U–Th determinations has been examined to relate the geomagnetic signature to earthquake-induced layering. Sequential sampling from the margins (earliest deposition) to the centres (last deposition) identifies directional migrations reminiscent of geomagnetic secular variation. On the assumption that these cycles record time periods of 1–2 ka, the number of travertine layers identifies resetting of the geothermal system by earthquakes every 50–100 years. Travertine precipitation occurs at rates of 0.1–0.3 mm a^{-1} on each side of the extensional fissures and at a rate an order higher than for bedded travertine on the surface. Earthquakes of magnitude $M \leq 4$ occur too frequently in the Sivas Basin to have any apparent influence on travertine deposition but earthquakes with M in the range 4.5–5.5 occur with a frequency compatible with the travertine layering, and it appears to be events of this order that are recorded by sequential travertine deposition. Two signatures of much larger earthquakes on a 1–10 ka time scale are also present in the travertine deposition: (1) the incidental emplacement of massive travertine or fracturing of earlier travertine without destruction of the fissure as a site of travertine emplacement; (2) termination of the fissure as a site of deposition with transfer of the geothermal activity to a new fracture. The presence of some 25 fractures in the *c*. 300 ka Sıcak Çermik field growing at rates of 0.1–0.6 mm a^{-1} suggests that the type (2) signature may be achieved by an M *c*. 7.5 event approximately every 10 ka.

The record of past earthquakes beyond historical and archaeological time scales relies on the identification of catastrophic events in the geological record. Movements along fault planes are the most direct signatures, with slickenlines indicating the latest sense of motion and offsets providing the cumulative movement of many successive events. Another effect is the liquefaction of incompetent sedimentary layers; this may provide evidence for ground shaking by earthquake events but cannot be used to constrain the events within a narrow time frame. The past directional behaviour of the Earth's magnetic field expressed in the short term (10^3–10^5 years) as palaeosecular variation (PSV) and occasional excursions, and in the long term (10^5–10^6 years) by reversals of polarity, can provide a time scale for ancient earthquakes provided that these same events are expressed in a rock succession with recoverable primary magnetism. The long-term changes in polarity may be linked to the Geomagnetic Polarity Time Scale (GPTS), whereas the archaeomagnetic and lake sediment records covering the last 10 ka years (Thompson & Oldfield 1986) suggest that PSV is closely constrained to the Earth's rotation with complete cycles taking 1000–2000 years to complete (Butler 1992).

Tectonically controlled travertine

The sedimentary deposit that most closely identifies earthquake events is tectonically controlled travertine. Travertine is inorganic carbonate deposition

From: TAYMAZ, T., YILMAZ, Y. & DILEK, Y. (eds) *The Geodynamics of the Aegean and Anatolia.* Geological Society, London, Special Publications, **291**, 291–305.
DOI: 10.1144/SP291.13 0305-8719/07/$15.00

and occurs whenever the partial pressure of CO_2 is reduced in waters draining hinterland including limestone and dolomites. In regions of neotectonism the groundwater is frequently at elevated temperatures, thus enhancing solution of country rock. These waters circulate to the surface via extensional fissures that become progressively filled by layers of travertine as they open (Hancock *et al.* 1999). Such fissures are typically banded because the hydrothermal system is episodically reset, and the flow stimulated, by earthquake activity. The incremental growth on each side of the fissure axis is then especially useful, because the layers are often variegated and can be correlated with one another to evaluate temporal trends in the geomagnetic record. The fissures feed layered travertine at the surface, where stratified deposits are produced by outflow onto the surface (Fig. 1). When travertine flow is tectonically controlled the stratified deposits at the surface may also be distinctively layered and alternate between slowly deposited friable, open-textured bands (tufa) and more massive, rapidly deposited bands. The friable bands are the product of waning hydrothermal activity as the conduits are progressively sealed by precipitation, whereas the massive bands result from stimulated flow after the reservoir has been fractured and reset by an earthquake event. Hence in regions of neotectonic activity travertine preserves a layered signature recording the past earthquake activity.

In this paper we report a palaeomagnetic study of fissure fill travertine from a geothermal field in central Turkey with the main aim of identifying migrations of the palaeofield direction to correlate with cycles of secular variation. As the travertine deposits also contain a history of layering, with each layer resulting from an earthquake event, we have aimed to evaluate the number of layers within secular variation cycles to estimate the long-term earthquake frequency. We also note two longer-term signatures in the travertine deposition, which appear to define the incidence of much larger but infrequent earthquake events.

Geological framework

The travertine examined in this study is derived from the geothermal region of Sıcak Çermik (39.9°N, 36.9°E) 25 km west of the city of Sivas in central Turkey where hot springs permeate Late Miocene–Early Pliocene sediments (Ayaz & Gökçe 1998). The carbonate source is probably marble in underlying metamorphic rocks lying >100 m below the sediments. The regional tectonic regime is dominated by NNW–SSE compression (σ_1) resulting from the continuing northward movement of Afro-Arabia into the Anatolides, an assemblage of accreted terranes between the Pontide orogen at the Eurasian margin in the north and the Tauride orogen in the south, although regional variations are complex, because of the westward extrusion of fault blocks within Anatolia (Tatar *et al*. 1996; Gürsoy *et al.* 1997; Piper *et al.* 2007). The axis of minimum principal stress (σ_3) is a tension in this region, and the sinuous pattern of fissure development (Fig. 2) suggests that it results from a torsional stress regime between two major NE–SW-trending tear faults so that only the currently active fissures are oriented NNW–SSE perpendicular to σ_3 (Mesci 2004). Quarrying of the mounds of layered travertine has excavated the sampled fissures and U–Th dating indicates that geothermal activity has occurred here, at least episodically, over the past 300–400 ka. The fissure fills consist of a succession of pale, straight, sinuous or undulating carbonate bands interrupted by darker bands of varying shades of brown; the more prominent examples of the latter can be reliably matched on either side of the fissure axes. The studied fissures are either completely sealed or are defined by a small gap showing that infilling by travertine occurred at approximately the same rate as the fissures were opened by the regional extension.

Palaeomagnetic study

Three travertine fissures at localities denoted 1, 2 and 3 in Figure 2 were drilled by coring outwards from the axes so that full thicknesses of travertine growth were sampled by successions of 2.4 cm diameter cores. At localities 1 and 2 suitable exposures allowed mirror sections to be sampled outwards on either side of the fissure axes. Orientations were by both Sun and magnetic compasses. Much of the layered travertine in this region comprises friable tufa and it was difficult to core coherent samples; isolated samples were obtained near the sampled fissures and at two sites (4 and 5) in more massive layered travertine, although the latter yielded few coherent data and are not further discussed here. Also, for comparative work, we have sampled 24 successive compact travertine layers from a travertine mound in a smaller geothermal field at Ortaköy near the town of Şarkışla 25 km SW of the Sıcak Çermik geothermal field.

The magnetizations in cores cut from field samples were determined by nitrogen SQUID (FIT) magnetometer following measurement of magnetic susceptibility using a Bartington Bridge. Progressive demagnetization was applied to resolve components of magnetization using either the alternating field (a.f.) method or thermal demagnetization. The preferred method of data analysis used orthogonal projections of the remanence vector onto horizontal and vertical planes accompanied by recognition of

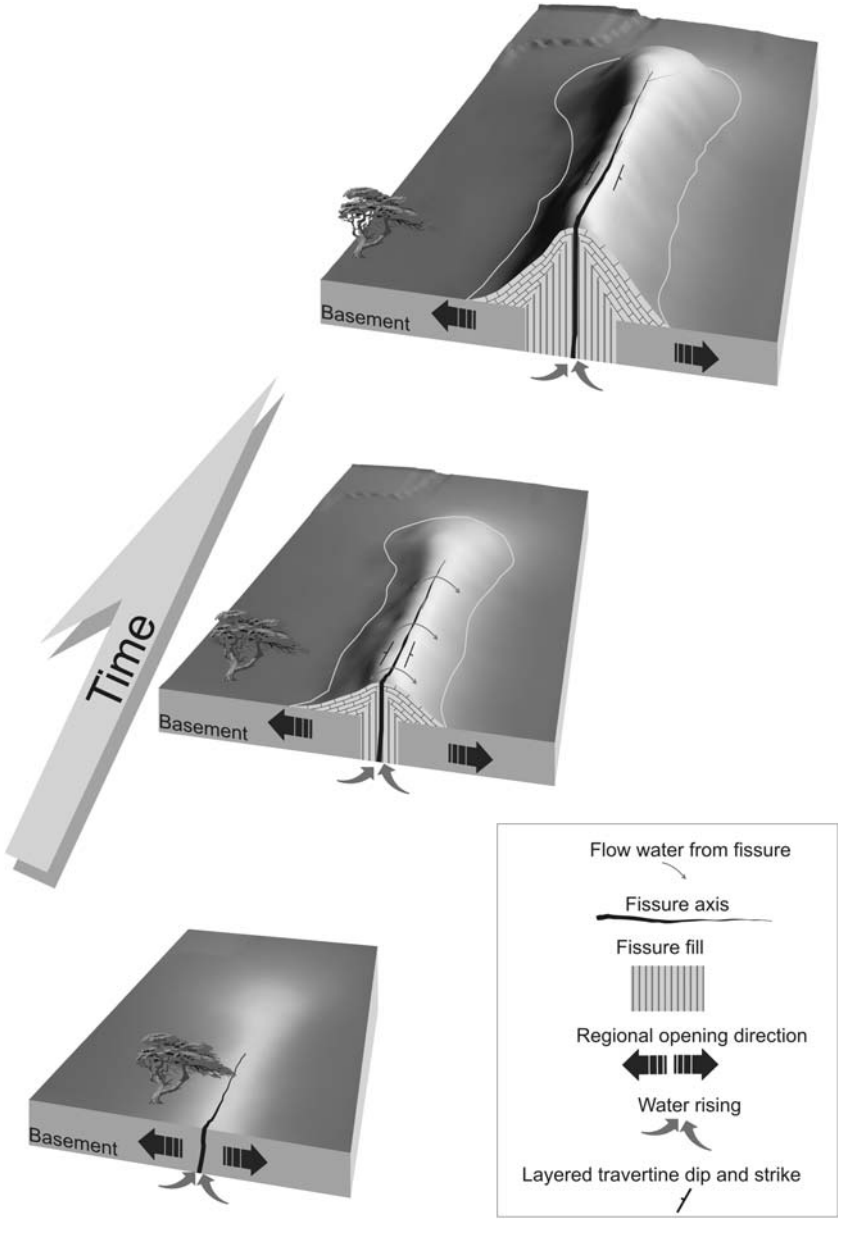

Fig. 1. The mode of formation of a travertine mound above an extensional fissure (after Mesci 2004).

components by eye and calculation of equivalent directions of magnetization by principal component analysis. Thermal demagnetization could be applied only to 350 °C because of disintegration of the carbonate host at higher temperatures, and directions of magnetization were determined by end-point analysis in samples showing stable behaviour where both methods of treatment produced minimal demagnetization trajectories.

Fissure locality 1

Fissure 1 is a 2 m wide example yielding U–Th ages of 120 000 ± 5 years at the axis and 177 000 + 14/−13 years at the margin (Mesci 2004). Figure 3 illustrates the sample distribution, comprising sites of 23 cores to the right of the axis (Site 1, west) and 26 cores to the left (Site 2, east). Thermomagnetic spectra show weak,

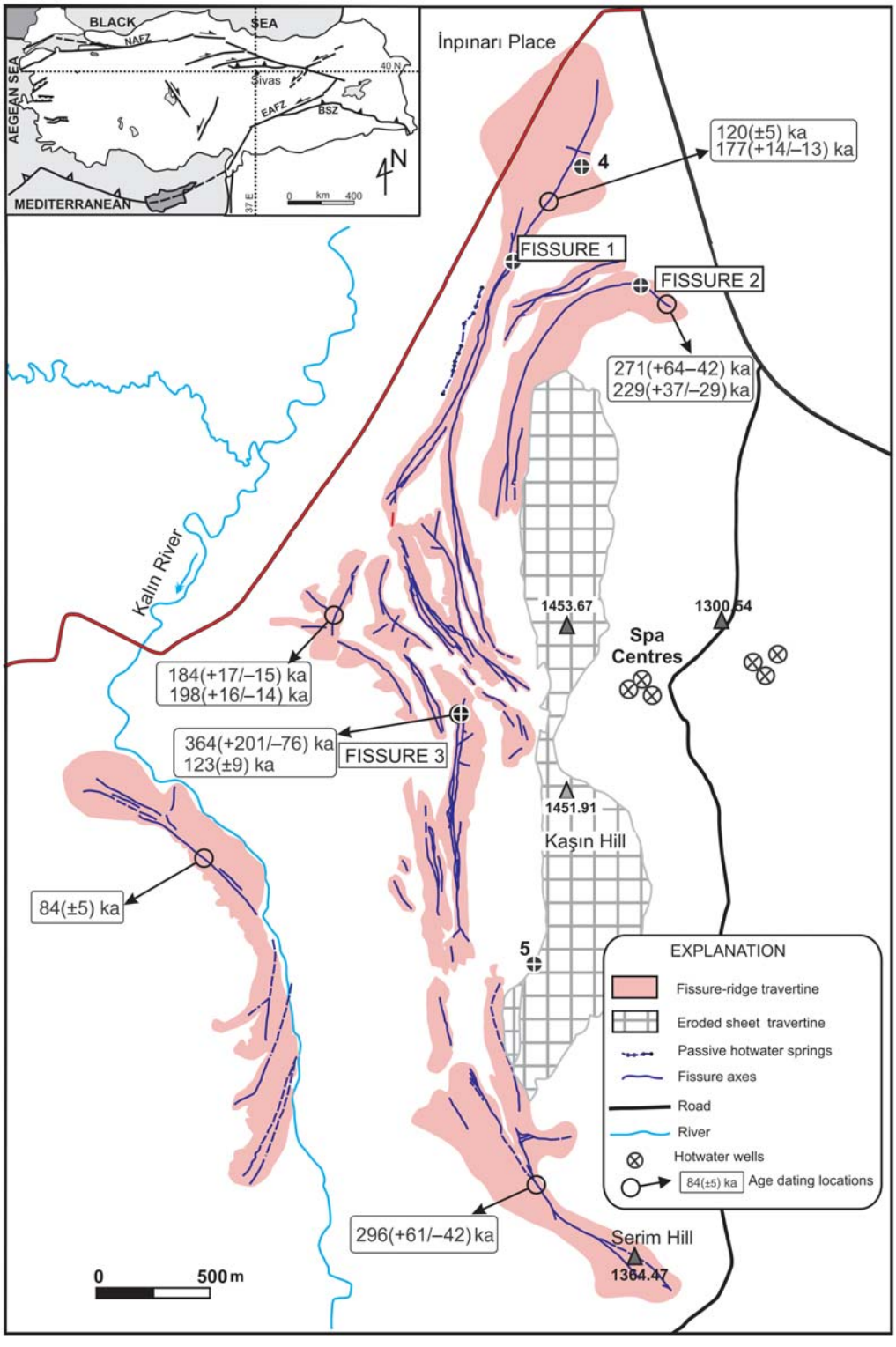

Fig. 2. Outline geological map of the Sıcak Çermik geothermal field near the city of Sivas, central Turkey. The locations of the three fissure travertines sampled for this study are shown, with two additional sites in bedded travertine (4 and 5). NAFZ, North Anatolian Fault Zone; EAFZ, East Anatolian Fault Zone; BSZ, Bitlis Suture Zone.

convex and asymptotic curves obeying the Curie Law; this indicates that saturation magnetization, M_s, is dominated by paramagnetism. Low-Ti magnetite is produced by alteration during heating, possibly from breakdown of siderite or reduction of limonite, and is reflected in large increase in M_s (Fig. 4). Acquisition of isothermal remanent magnetization (IRM) shows continuing rise of curves to the limits of laboratory fields (2.7 T) and identifies much of the ferromagnetism in these rocks as due to goethite or hematite (Fig. 4). The travertine has a weak remanence that is measurable following a.f. demagnetization in steps ranging from 2.5–20 mT to peak fields of 130 mT. Examples of orthogonal projections are illustrated in Figure 5. Components defining directions with mean angular deviations of $\leq 25^\circ$ were accepted and successive mean directions of magnetization were calculated from threefold running means from successive cores to evaluate directional trends across the fissure.

Magnetic declinations on the left- and right-hand sides of the fissure show similar variation, with a swing of the palaeofield initially to the east, then to the west, and finally back to the east (Fig. 6). The inclination records also correspond very closely out to sample 12, but beyond this point they diverge, with site 1 becoming steeper and site 2 shallower than the mean field inclination in this region. The variation in declination is of higher frequency than the variation in inclination; this same contrast is present, for example, in the historical PSV record in Europe (e.g. Marton 1996). The mean direction yielded by the running means of the samples from site 1 on the west side of the fissure axis is $D/I = 348.7/58.7^\circ$ ($N = 18$, $R = 17.21$, $\alpha_{95} = 7.6^\circ$, $k = 21.5$) and from site 2 on the east side of the axis is $D/I = 345.2/56.0^\circ$ ($N = 18$, R = 16.93, $\alpha_{95} = 8.9^\circ$, k = 15.9). The inclinations are not significantly shallower than the inclination predicted from the geocentric axial dipole field at the sample locality ($I = 59^\circ$). The declinations, however, appear to be rotated anticlockwise from north, consistent with the interpretation that the fissure system in this geothermal field is undergoing torsional rotation between bounding ENE–WSW strike-slip faults as a consequence of the tectonic escape of terranes in central Anatolia (Mesci 2004). Beyond sample 18 (Fig. 3) it is not possible to correlate bands on either side with confidence and beyond core 21 in site 1 the layering is truncated at the base of the outcrop, with older layers apparently recording a separate period of growth. We infer that a rare larger earthquake event occurred at this point, which dislocated the fissure but was not of sufficient magnitude to destroy the fissure as a conduit for water flow.

The time sequence of mean directions of magnetization show a net clockwise migration (Fig. 7), the anticipated response of the magnetic vector to the westward motion of a magnetic dipole in the Earth's core and consistent with well-known

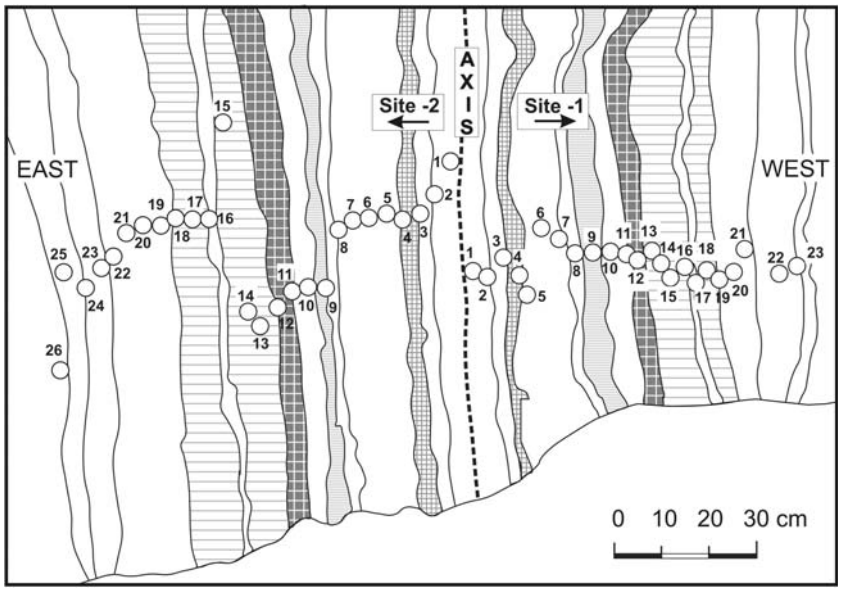

Fig. 3. Drawing from a photograph of fissure 1 at Sıcak Çermik, showing the system for sampling the palaeomagnetic cores across a fissure travertine.

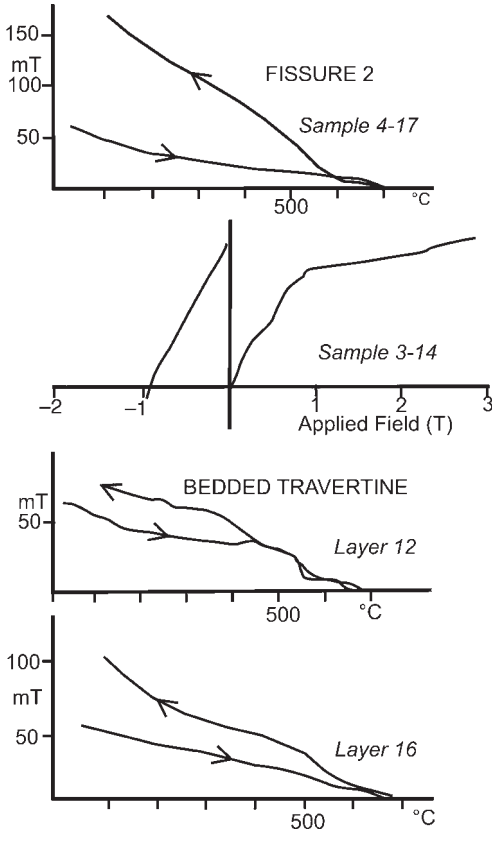

Fig. 4. Typical thermomagnetic (saturation magnetization (M_s) v. temperature) determinations and IRM acquisition curves for samples of fissure and bedded travertine.

European observatory data. Some 60 cm of travertine growth at this locality thus appear to be just short of recording a complete cycle of secular variation. Analogies with the historical field and the lake sediment record (Butler 1992) suggest that some 2000 years of deposition could be represented, and suggest a rate of carbonate incrementation of *c.* 0.3 mm a^{-1}. Approximately 50 layers are discernible within this thickness and suggest that earthquakes large and/or close enough to reset the reservoir and stimulate water flow occurred roughly every 40 years. At this locality the record of PSV thus suggests a fissure lifespan much shorter than the 177–120 ka interval suggested by the U–Th determinations; we address this discrepancy below in the context of the data from fissures 2 and 3.

Fissure locality 2

This is a *c.* 3 m wide fissure dated by U–Th at $271 + 64/-42$ ka at the axis and $299 + 37/-29$ ka at the margin (Mesci 2004). The palaeomagnetic sample comprises 49 cores from the east side (site 3) and 43 cores from the west side (site 4). The cores were subjected to a.f. demagnetization incremented in 5 mT steps to 35 mT and then in steps of 50, 75, 100 and 140 mT. All samples were characterized by high magnetic coercivities but this treatment was usually able to subtract sufficient remanence to demonstrate convergent vectors and identify single-component behaviours. Component directions fall into two groups: the majority of cores show directions close to the present field direction with small consecutive directional change between adjacent cores. The remainder show directions diverging widely from the recent field direction although approximately consistent between adjacent cores until there is a shift back to the predicted field direction. The outer parts of this fissure (core 28 and beyond) shows thin parallel layers of travertine that can be readily correlated on either side. Comparable swings in declination and inclination can be identified in this part of the fissure (Fig. 8) and suggest that one full cycle of PSV is recorded within this initial (outer) sequence

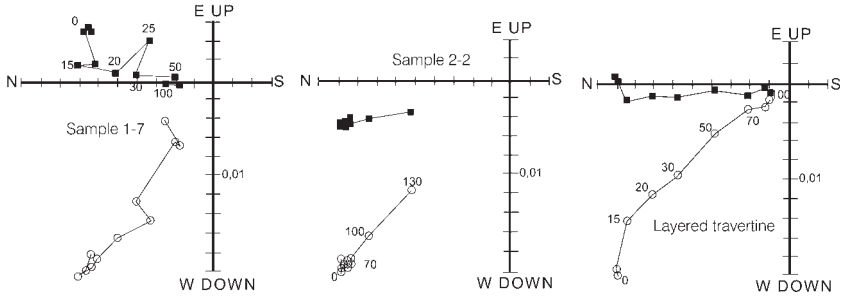

Fig. 5. Typical orthogonal projections of the magnetization vector during a.f. demagnetization from fissure travertine at sites 1 and 2 in fissure 1 and an example of demagnetization of bedded travertine bordering this fissure. Projections onto the horizontal plane are shown as filled symbols and projections onto the vertical plane are shown as open symbols. The intensity values are $\times 10^{-5}$ A m^2 kg^{-1}.

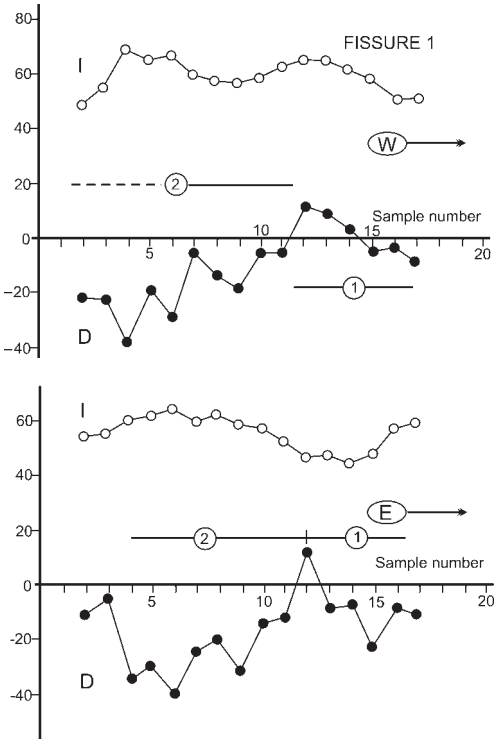

Fig. 6. Variation in the declination and inclination of the magnetization on each side of the axis of fissure 1.

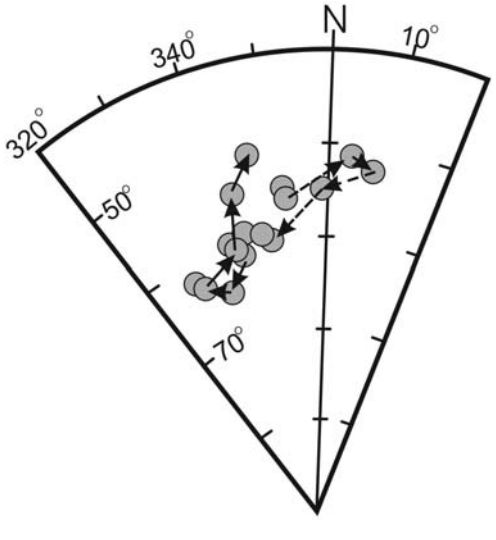

Fig. 7. Directional migration of the geomagnetic field recorded by successive travertine growth in fissure 1.

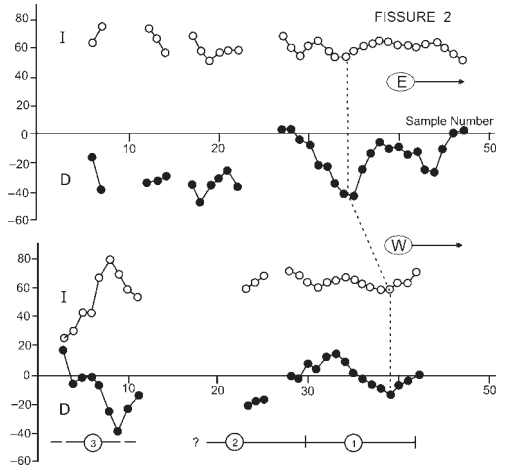

Fig. 8. Variation of the magnetic declination and inclination recorded by travertine growth across fissure 2.

of travertine deposition. Only fragments of a subsequent cycle were recorded although the last pulse of deposition recorded approximately half a cycle of PSV before the fissure became extinct. The initial phase of layered travertine (about 1.5 cycles of PSV) records 31 layers of travertine whereas the last (half-cycle) records eight layers. In each case the deposition of one travertine layer in *c*. 100 years is indicated and a rate of travertine growth of *c*. 0.2 mm a^{-1} is implied.

Thirty-eight of 47 samples from site 3 having directions comparable with the recent field yield a mean direction of $D/I = 339.8/60.3^{\circ}$ ($R = 36.99$, $k = 36.6$, $\alpha_{95} = 3.9^{\circ}$) whereas 28 of 42 samples from site 4 have a mean of $D/I = 356.8/60.3^{\circ}$, $R = 26.85$, $k = 23.4$, and $\alpha_{95} = 5.8^{\circ}$). Thus the mean field inclination recorded here is not significantly different from the geocentric dipole value of 59°. The declination, however, is rotated anticlockwise by a similar amount to the declination in fissure 1.

The incomplete recovery of an interpretable field direction correlates with the presence of travertine banding with contorted shapes and with massive (unbanded) travertine within the inner part of the fissure (Fig. 9), which has only incidentally recorded the predicted field. It appears that precipitation processes within the fissure during turbulent flow or incidental catastrophic events prevented recording of the ambient field direction; hence this kind of travertine would appear to be unsuitable for investigation of PSV. Because of the insertion of this massive travertine into this fissure we are unable to estimate the duration of activity but on the assumption that it spanned about three cycles of PSV, it could be of the order

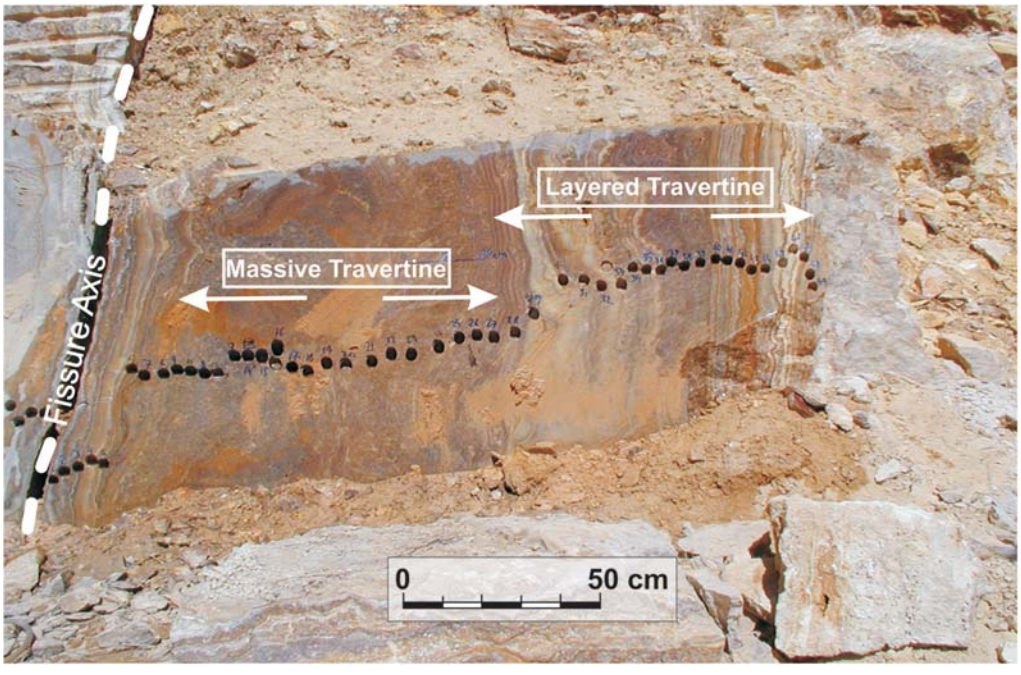

Fig. 9. Photograph of fissure 2 (eastern side) showing the distribution of palaeomagnetic samples and three types of fissure travertine: uniformly layered travertine, convolute layered travertine and massive (non-layered) travertine.

of 5000 years, which is within the margin of error of the U–Th age determinations from the margin and axis noted above. Between 60 and 65 bands are discernible (uncertainties arise as a result of local truncation) between the axis and the outer core, suggesting that resetting of the reservoir by earthquake activity occurred approximately every 80 years. The average carbonate incrementation of the *c*. 145 cm of travertine sampled on each side of the fissure is *c*. 0.3 mm a^{-1}; however, this value is biased by the massive travertine layer and a more realistic estimate for the rate of growth of the banded travertine is the value of 0.2 mm a^{-1} noted above.

Fissure locality 3

This is a wide fissure dated by U–Th analysis at 123 ± 9 ka at the axis and $364 + 201/-76$ ka at the margins (Mesci 2004). It is the widest fissure investigated here, although it was cored on one side only so we are unable to compare growth on either side of the axis.

The cores in this example were treated by thermal demagnetization to determine whether the ferromagnet goethite, presumed to be a component of the brown colour of much of the travertine, is a significant remanence carrier. Thermal demagnetization could then surmount the difficulty that coercivities are very high in most of the travertine samples and component trajectories are correspondingly difficult to define. Because goethite has a Curie point of only *c*. 125 °C, steps of only 25 °C were used commencing at 50 °C and continuing to 150 °C. In the event, only marginal reduction of the remanent intensity of 5–10% had been achieved by this temperature, thus showing that hematite rather than goethite must be the carrier of the high-coercivity remanence identified by a.f. demagnetization. The thermal demagnetization was continued in 50 °C steps until the carbonate began to disintegrate at *c*. 350 °C, and this achieved variable reduction in natural remanent magnetization, which often allowed convergent vectors to be recognized and defined.

To illustrate the effect of calculating successive three-point means to determine palaeofield migration across a fissure we show both the raw and smoothed data for declination in Figure 10 and for inclination in Figure 11. Continuing to adopt the criteria that a swing in declination and/or inclination is significant only if it is recognized in more than one successive sample, we identify five complete cycles of PSV across this fissure. These are evident in both the raw and smoothed data (Fig. 10), with the chief uncertainty being

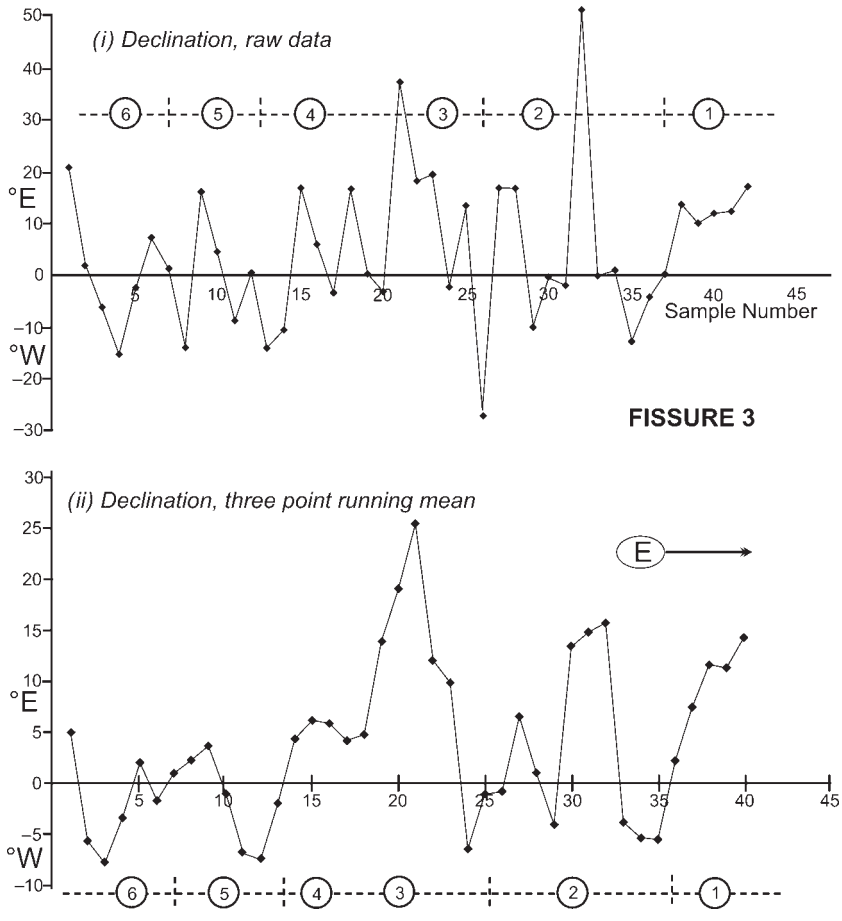

Fig. 10. Variation of the magnetic declination recorded by travertine growth across fissure 3. Both raw data and Fisherian means derived from applying a three-point filter are shown.

within cycles 3 and 4, where three counter-clockwise swings in declination are observed although the complementary clockwise swing is defined with confidence only in the earlier part of cycle 3. As in fissure 1, declination changes are higher in frequency and magnitude than inclination changes. Approximately 85 layers are discernible across this fissure as distinct white or brown bands, and indicate an earthquake event large enough to reset the reservoir approximately every 120 years. The rate of travertine growth appears to have been *c*. 0.1 mm a^{-1}.

Bedded travertine (Ortaköy geothermal field)

A comparative sample of layered travertine has been collected from the Ortaköy geothermal field located SW of Sıcak Çermik and comprises 24 successive layers derived from a single travertine mound. The basal layer overlies volcanoclastic sediments and a 2 m thick basal layer of massive and brecciated travertine. Succeeding layers range from 14 to 50 cm in thickness and make up a total thickness of 7.9 m to the summit of the mound. This deposit is undated, although geothermal activity is present nearby and it is likely to be no more that a few tens of thousands of years old. Two samples were drilled from each layer and used to derive layer means summarized in Table 1.

Mean declinations and inclinations are summarized as a log in Figure 12 and compared with magnetic susceptibility through the same section. All but two layers (8 and 20) yielded measurable and stable components of magnetization, although only one core at layers 1 and 20 yielded useful data. Layer mean directions summarized in Table 1 show typical normal polarity fields with declinations ranging from 324°E to 9°E and

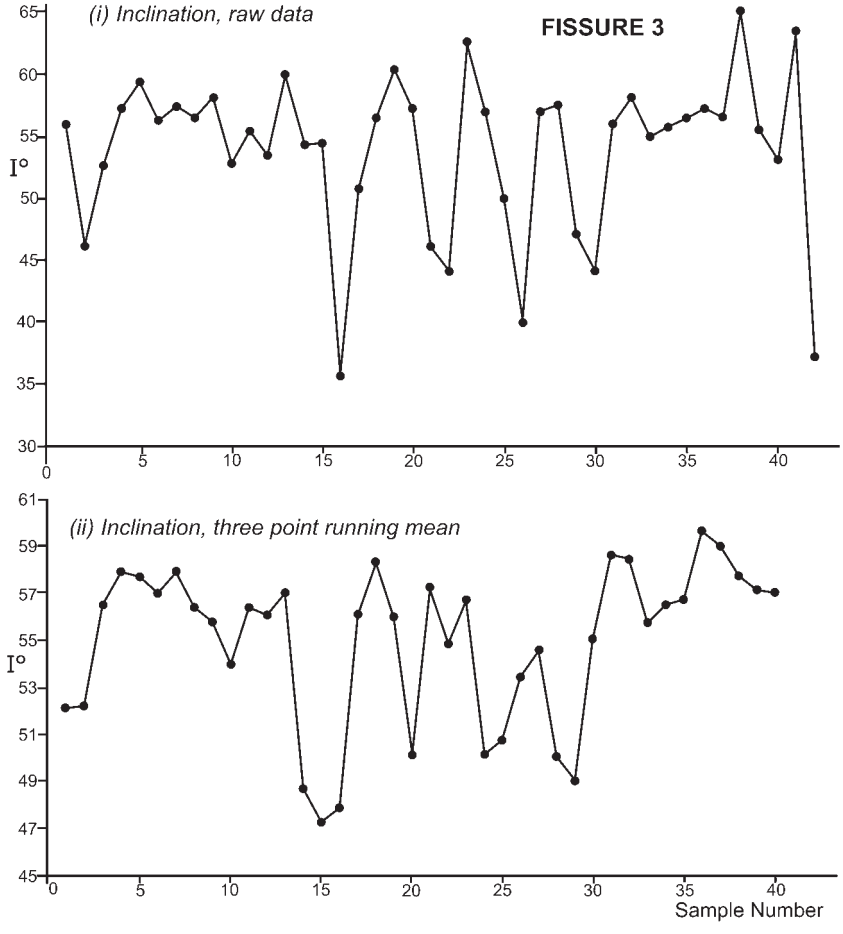

Fig. 11. Variation of the magnetic inclination recorded by travertine growth across fissure 3. Raw data and Fisherian means derived from applying a three-point filter are shown for comparison.

inclinations ranging from 34° to 66°. The mean direction derived from 20 layer means is $D/I = 353/47°$ ($\alpha_{95} = 5.2°$). Thus the significance of the direction of magnetization in this bedded travertine contrasts with the results from the fissure travertines: the declination barely differs from the mean ambient field direction within confidence limits although a small anticlockwise rotation consistent with the pattern of declinations across central Anatolia is possible (Gürsoy *et al.* 1997). In contrast, the inclination is notably shallower than the inclination (58.5°) predicted at this latitude (39.4°N) from a geocentric axial dipole source. Because no inclination shallowing is observed in the fissure travertine, this suggests that a depositional mechanism is responsible for this effect in bedded travertine; a likely mechanism is the settling of elongate and platy shaped ferromagnetic grains (Butler 1992) as they settle through the water films to become incorporated into the precipitating carbonate.

Earthquake frequency here has not been high enough to reset the hydrothermal system and deposit sufficient layers to record cycles of secular variation with complete confidence (although multiple layers between 2 and 3 were too thin to sample) and there are two possible interpretations of these data. First, the surface bedded travertine with an open porous texture is likely to be more susceptible to diagenesis than the compact and impervious fissure travertine and the magnetic record may be more susceptible to alteration by continuing fluid drainage. In these circumstances no consistent record of PSV might be recorded in layered travertine. Second, however, it is possible that detrital ferromagnetic grains could be fixed in the host carbonate and still be essentially impervious to significant later change. Thus if we exclude declination

Table 1. *Summary of palaeomagnetic results from bedded travertine deposit at Ortaköy, SW of Sivas, central Turkey*

Layer number	*D*	*I*	*N*/*R*	α_{95}
1	(348.5)	(49.5)	1/–	
2	5.8	41.1	2/2.00	6.7
3	348.6	50.3	2/2.00	2.2
4	354.6	44.7	2/2.00	10.6
5	359.6	51.6	2/2.00	7.8
6	22.4	53.4	3/2.99	8.3
7	1.6	47.7	2/1.98	32.2
8	–	–	–	–
9	6.2	47.2	2/1.98	35.2
10	338.0	34.7	2/2.00	9.9
11	346.4	36.2	4/3.96	10.8
12	223.9	33.8	2/1.99	24.5
13	2.6	36.4	2/2.00	3.5
14	327.9	51.8	3/2.94	22.1
15	338.9	40.7	3/2.97	14.6
16	358.8	39.6	2/2.00	13.1
17	349.0	48.1	2/1.99	22.8
18	6.2	48.3	2/1.99	19.7
19	8.9	59.3	2/1.99	24.6
20	–	–	–	–
21	(347.2)	(65.6)	1/–	
22	329.1	51.7	3/2.96	16.9
23	358.0	53.5	3/3.00	4.5
24	352.7	49.1	2/2.00	7.8
Mean result (20 layers)	353.4	46.9	20/19.50	5.2

Pole position is 77°N, 248°E ($dp/dm = 4.3/6.7°$).

and inclination swings defined by single layers only, it appears that two complete cycles of PSV are recorded by the log in Figure 12 so that some 2000–4000 years of deposition are represented here, with each layer (and equivalent earthquake cycle) recording intervals of the order of 100–200 years. Deposition rates of the travertine would then have been 2–4 mm a^{-1}. This is about an order higher than the rate of deposition of the layered fissure travertine at Sıcak Çermik and is consistently explained by the following: (1) the carbonate-charged water is preferentially blown forcibly out of the fissure by activity of the steam; (2) the largest reduction in PCO_2 takes place at the surface; (3) it is here that the water moves away only slowly and is subject to strong evaporation.

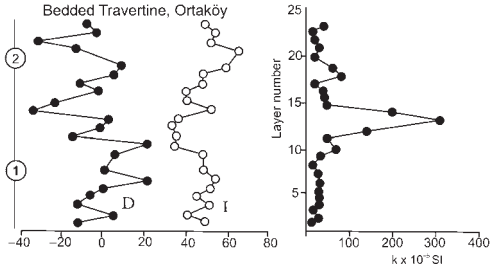

Fig. 12. Variation of magnetic declination and inclination derived from palaeomagnetic study of 24 successive layers through bedded travertine in the Ortaköy geothermal field. Also shown is the variation of magnetic susceptibility through this succession.

Of especial interest is the large increase in magnetic susceptibility observed between layers 11 and 15 (Fig. 11). The dramatic input of magnetic material at this point could have several possible explanations including: (1) the signature of a volcanic event; (2) a change in groundwater chemistry; (3) a change in the principal wind direction carrying enhanced magnetic detritus into the region. Because the enhanced susceptibility is recognized through three successive layers the time period involved is likely to have been several hundreds of years, and explanations (2) or (3) are therefore more likely. Volcanic outcrops are extensively exposed in the immediate vicinity of Ortaköy and are a possible source of wind-borne magnetite. Volcanic rocks around the town of Ortaköy were regarded as Pliocene–Pleistocene by Parlak *et al.* (2001) although K–Ar age dating of basalts by Tatar *et al.* (2004) has yielded a somewhat older age of 12.96 ± 0.10 Ma.

Table 2. *Historical earthquakes affecting central Anatolia*

Date	Magnitude	Number of deaths	Affected area	Origin
240	?	?	Kayseri–Sivas	CAFZ?
1205	?	?	Kayseri	CAFZ?
1268	?	15000	Erzincan–Erzurum	CAFZ?
1458	?	30000	Erzincan–Erzurum	CAFZ?
17.08.1668	?	?	Amasya–Tokat–Sivas	CAFZ?
11.01.1695	?	?	Sivas–Ordu	CAFZ?
06.09.1704	?	?	Kayseri	CAFZ?
1714	?	?	Kayseri	CAFZ?
09.05.1717	?	8000	Kayseri	CAFZ?
16.09.1754	?	?	SE Sivas	CAFZ?
14.03.1779	?	?	Divriği–Malatya	Malatya Fault?
28.05.1789	?	?	Divriği–Elazığ	Malatya Fault?
18.07.1794	?	?	Central Anatolia	NAFZ
02.06.1859	6.4	15000	Erzurum	?
10.1891	6 (I_o)	?	Sivas and Hafik	?
1893	6 (I_o)	?	Sivas and Zara	?

After data compiled from Ergin *et al*. (1967), Ambrasseys & Finkel (1995) and Boğaziçi University Kandilli Observatory and Earthquake Research Institute, Istanbul.
CAFZ, Central Anatolian Fault Zone; NAFZ, North Anatolian Fault Zone.

Table 3. *Earthquakes with magnitude >3 (M_s) that occurred between 1900 and 2005 in and around the study area*

Date	Time (GMT)	Latitude (°N)	Longitude (°E)	Depth (km)	Magnitude (M_s)
25.12.2005	03:50	39.64	37.33	8	3.3
12.10.2005	04:12	39.72	37.43	3	3.1
27.09.2005	05:24	39.70	37.30	25	3.1
06.08.2005	18:34	39.68	37.47	20	3.3
14.12.2004	22:49	39.77	36.75	5	3.2
14.12.2004	22:24	39.77	36.74	5	4.1
09.03.2004	12:39	39.43	37.32	3	3.2
02.02.2004	02:08	39.51	37.01	5	3.4
08.01.2004	22:28	39.39	37.01	13	3.1
26.11.2003	01:17	39.48	36.67	5	3.0
09.08.2003	15:07	39.76	37.44	5	3.4
18.06.2002	08:08	39.70	37.45	5	4.0
11.06.1999	05:44	39.53	36.83	9	4.0
11.06.1999	05:25	39.49	36.67	10	4.8
15.12.1998	20:15	38.96	35.81	8	4.1
14.12.1998	13:06	38.95	35.72	5	4.6
14.12.1998	12:44	38.96	35.91	6	4.3
31.07.1995	03:26	39.51	36.48	0	4.5
23.01.1985	01:23	39.11	35.94	33	4.6
31.08.1960	22:11	39.09	35.98	70	4.7
12.03.1960	21:25	39.40	36.40	0	4.5
07.06.1940	19:49	40.06	37.82	10	4.6
27.12.1939	02:48	39.99	38.14	50	5.5
28.06.1929	22:18	40.20	37.90	0	4.5
18.05.1929	06:37	40.20	37.90	10	6.1
10.02.1909	19:49	40.00	38.00	0	5.7
09.02.1909	14:38	40.00	38.00	0	5.8
09.02.1909	11:24	40.00	38.00	60	6.3

After Boğaziçi University Kandilli Observatory and Earthquake Research Institute, Istanbul.

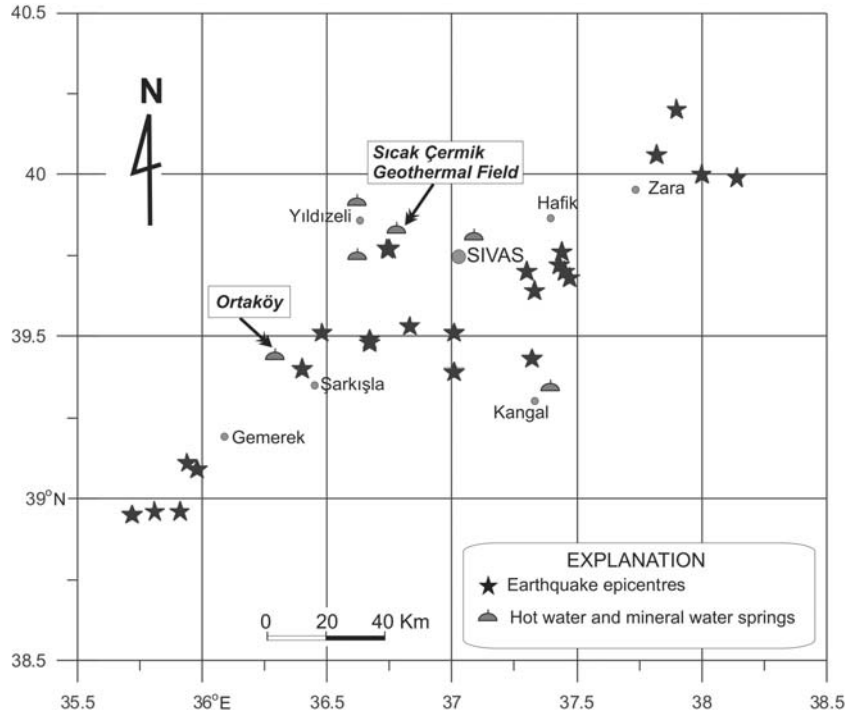

Fig. 13. The region of the Sivas Basin bordering the Sıcak Çermik geothermal field, showing epicentres of $M \geq 4$ 20th century earthquakes.

Discussion

Although the U–Th dating results are able to show that geothermal activity in the Sıcak Çermik field has spanned the last 300–400 ka, they are unable to constrain the intervals of activity within individual fissures with much precision. There are some 25 fissures in this geothermal field (Fig. 2) and, on the assumption that fluid outflow was concentrated on one fissure at a time, they may have been active for *c*. 12 ka on average, although this estimate will be a minimum because more than one fissure might have been active at any one time. The signature of PSV within the three fissures studied here implies activity over significantly shorter intervals than this. However, this discrepancy is more apparent than real because the full history of fissure growth is recorded only at the base of each fissure mound (Fig. 1); as the travertine pile builds up the fissure advances through successive layers so that the highest parts record only the last phase of activity of the fissure. Hence the interval of PSV recorded within a fissure will be controlled by the depth of exposure and the level of sampling.

Historical seismic activity in the Sivas Basin has been included in the assessments of a number of researchers (e.g. Gençoğlu *et al.* 1990; Ambraseys & Jackson 1998; Table 2). Damaging earthquakes were also noted in Sivas in 1695 and in the Kayseri district to the SW in *c*. 1745 (Ambraseys & Finkel 1995). A greater frequency of smaller earthquakes is evident from the high density of normal faults cutting Quaternary alluvial deposits bordering the adjoining Kızılırmak River (Gürsoy *et al.* 1992). Earthquake epicentres highlight a NE–SW trend of major faults delineating block boundaries and recording predominantly strike-slip motions resulting from the southwestward extrusion of terranes in central Anatolia by tectonic escape (Fig. 12). Most recently, Mesci (2004) has compiled a record of observatory recorded earthquakes and identified more than 50 earthquakes of $M \leq 4$ between 1995 and 2002 (Table 3; Fig. 13). Clearly, earthquakes of this magnitude occur much too frequently to have significantly influenced travertine formation. Twelve earthquakes with magnitudes between 4 and 4.8 occurred between 1929 and 2005 and five earthquakes with magnitudes between 5.5 and 6.3 occurred between 1909

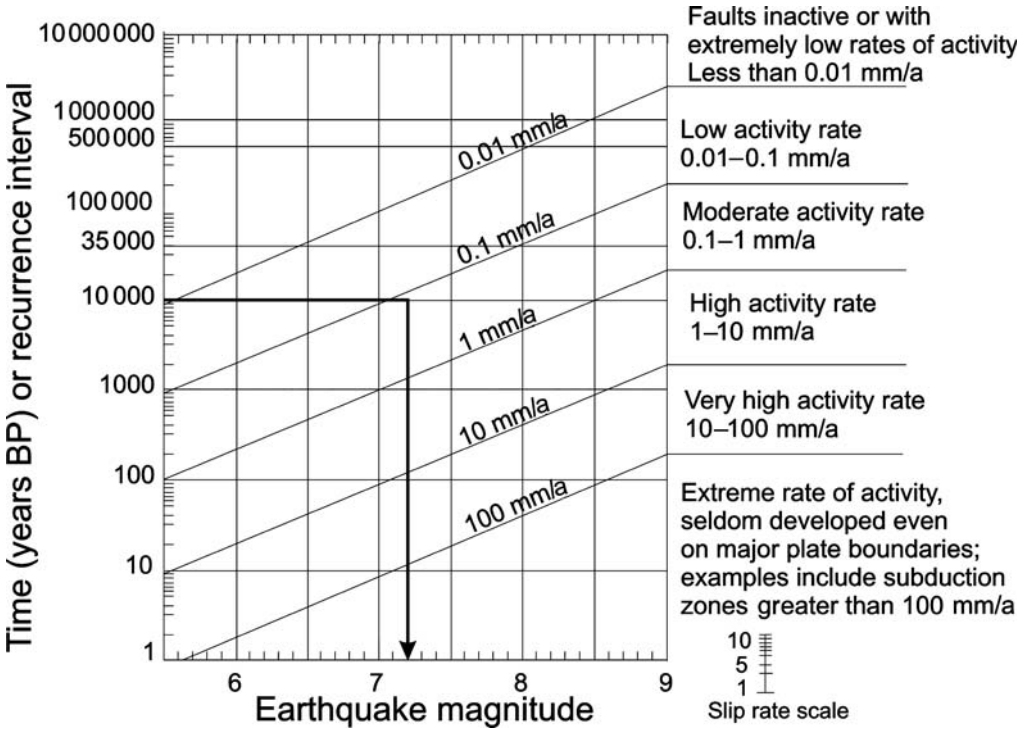

Fig. 14. The relationship between earthquake magnitude and fault offset used to estimate the recurrence time of earthquakes in western North America. After Schwartz & Coppersmith (1984) and Keller & Pinter (1996).

and 1939. Because only a few of these events would have occurred sufficiently close to influence the geothermal field, it seems likely that events in the magnitude range *c*. 4.5–5.5 are those capable of resetting the reservoir and instigating a revitalized water flow.

There are two further signatures within the record of travertine deposition in this geothermal field for the incidence of less frequent but much larger earthquakes. The first is the incidental emplacement of massive travertine without destroying the fissure as a site of travertine emplacement, such as that observed in the central part of the record at fissure 2, and perhaps the truncation of the outer record of the travertine in fissure 1 noted above. The second is the termination of the fissure as a site of deposition with transfer of the geothermal activity to a new fracture. A tentative estimate of the earthquake magnitude and frequency responsible for the second and most catastrophic type of earthquake event can be made from the relationship between earthquake magnitude and fault offset used to estimate the recurrence time of earthquakes in western North America (Schwartz & Coppersmith 1984). This approach is valid provided that repeated earthquakes on the fault segment occur with approximately the same magnitudes and amounts of displacement. The earthquake model assumes that the slip rate of the fault, the magnitude of the earthquake and the displacement per event are related in a systematic way. The model of Schwartz & Coppersmith relates the average recurrence time to the ratio of the displacement per event and the slip rate, on the assumption that an M = 7 earthquake is characterized by a 1 m displacement, an M = 8 event by a 5 m displacement, etc. The relationships for this example are shown in Figure 14 after Keller & Pinter (1996). In the Sıcak Çermik field the palaeomagnetic results show that the fissures have grown at rates of 0.1–0.3 mm a^{-1} on either side and have active durations of a few thousand years. As noted above, our samples will have embraced a significant part, but not the whole, of the history of each fissure, so an average lifespan of *c*. 10 ka is a reasonable estimate. Entering these values into the empirical relationship of Keller & Pinter (1996) suggests that an M = 7.5 event every *c*. 10 ka could record the extreme of earthquake activity in this region and be responsible for shifting the geothermal activity to a new fracture.

Conclusions

This investigation has been mainly exploratory in nature and designed to determine whether travertine, the natural deposit most closely linked to the regional earthquake signature, can yield a palaeomagnetic record of value to palaeoseismological investigation. In the event, it has been found that both fissure and bedded travertine yield an accurate record of the palaeomagnetic field direction and illustrate progressive changes in direction compatible with the signature of PSV. The record in bedded travertine is less clearly related to PSV than the record in fissure travertine and may be influenced by diagenesis; the value of bedded material for palaeoseismological investigation thus requires more investigation. The temporal link to earthquake frequency is based on the assumption that cycles of PSV were similar to those resolved from archaeological and historical records during the past few thousand years. By counting the number of travertine layers within a cycle of PSV we have a means of estimating the frequency of earthquakes capable of resetting the reservoir. The rate of travertine growth is also determined, as well as the nature of PSV. The typical magnitudes of the earthquake events responsible for influencing the travertine deposition can then be estimated from the historical records.

Two larger but more incidental signatures of earthquake activity are recorded in travertine deposits and suggested by the occasional emplacement of massive travertine and by the initiation of new travertine fissures. Travertine can thus provide an indication of bimodality in earthquake magnitude or frequency and indicate sourcing from two or more levels and stress regimes within the crust.

We are grateful to the British Council, NATO (Grant No. CLG-EST-977055) and TÜBİTAK (Grant YDABAG 101Y023) for supporting palaeomagnetic and neotectonic investigations in Turkey and for promoting the link between the Department of Geology at the Cumhuriyet University and the Geomagnetism Laboratory at Liverpool. We are grateful to E. Bozkurt and C. Yaltırak for reviews and for advice that improved the manuscript, and to T. Taymaz for editorial help.

References

AMBRASEYS, N. N. & FINKEL, C. F. 1995. *Seismicity of Turkey and Adjacent Areas: an Historical Catalogue of Earthquakes 1500–1799*. Eren, Istanbul.

AMBRASEYS, N. N. & JACKSON, J. A. 1998. Faulting associated with historical and recent earthquakes in the Eastern Mediterranean region. *Geophysical Journal International*, **133**, 390–406.

AYAZ, E. & GÖKÇE, A. 1998. Geology and genesis of the Sıcak Çermik, Sarıkaya and Uyuz Çermik travertine deposits northwest of Sivas, Turkey. *Bulletin of the Faculty of Engineering, Cumhuriyet University, A*, **15**, 1–12.

BUTLER, R. F. 1992. *Palaeomagnetism: Magnetic Domains to Geologic Terranes.* Blackwell, Oxford.

ERGIN, K., GÜÇLÜ, U. & UZ, Z. 1967. *Türkiye ve Civarının Deprem Kataloğu*. İTÜ, Maden Fakültesi Yayınları, **24**.

GENÇOĞLU, S., İNAN, E. & GÜLER, H. H. 1990. *Tükiye'nin Deprem Tehlikesi.* Chamber of Geophysical Engineering of Turkey, Ankara.

GÜRSOY, H., TEMIZ, H. & POISSON, A. 1992. Recent faulting in the Sivas area (Sivas Basin, Central Anatolia—Turkey). *Bulletin of the Faculty of Engineering, Cumhuriyet University, A*, **9**, 11–17.

GÜRSOY, H., PIPER, J. D. A., TATAR, O. & TEMIZ, H. 1997. A palaeomagnetic study of the Sivas basin, Central Turkey: crustal deformation during lateral extrusion of the Anatolian block. *Tectonophysics*, **271**, 89–105.

HANCOCK, P. L., CHALMERS, R. M. L., ALTUNEL, E. & CAKIR, Z. 1999. Travitonics: using travertines in active fault studies. *Journal of Structural Geology*, **21**, 903–916.

KELLER, E. A. & PINTER, N. 1996. *Active Tectonics.* Prentice–Hall, Englewood Cliffs, NJ.

MARTON, P. 1996. Archaeomagnetic directions: the Hungarian calibration curve. *In*: MORRIS, A & TARLING, D. H. (eds) *Palaeomagnetism and Tectonics of the Mediterranean Region.* Geological Society, London, Special Publications, **105**, 385–399.

MESCI, B. L. 2004. *The development of travertine occurrences around Sıcak Çermik (Sivas) and their relationship with active tectonics.* PhD thesis, Cumhuriyet University, Sivas.

PARLAK, O., DELALOYE, M., DEMIRKOL, C. & ÜNLÜGENÇ, U. C. 2001. Geochemistry of Pliocene–Pleistocene basalts along the Central Anatolian Fault Zone. *Geodinamica Acta*, **14**, 159–167.

PIPER, J. D. A., TATAR, O., GÜRSOY, H., KOÇBULUT, F. & MESCI, B. L. 2007. Paleomagnetic analysis of neotectonic deformation in the Anatolian accretionary collage, Turkey. *In*: DILEK, Y. & PAVLIDES, S. (eds) *Postcollisional tectonics and magmatism in the Mediterranean region and Asia*. Geological Society of America, Special Paper, **409**, 417–439.

SCHWARTZ, D. P. & COPPERSMITH, K. J. 1984. Fault behaviour and characteristic earthquakes: examples from the Wasatch and San Andreas Fault Zones. *Journal of Geophysical Research*, **89**, 5681–5698.

TATAR, O., PIPER, J. D. A., GÜRSOY, H. & TEMIZ, H. 1996. Regional significance of neotectonic anticlockwise rotation in central Turkey. *International Geology Review*, **38**, 692–700.

TATAR, O., TEMIZ, H., GÜRSOY, H. & GUEZOU, J. C. 2004. *Orta ve Kuzey Anadolu Miyosen-Kuvaterner volkanizması ışığında Avrasya-Anadolu levhalarının çarpışması.* TÜBİTAK Projesi, No. **YDABÇAG-198Y092**.

THOMPSON, R. & OLDFIELD, F. 1986. *Environmental Magnetism.* Allen & Unwin, London.